Respiratory motion prediction for adaptive radiotherapy

Abdelhamid Sahih, Olivier CL Haas, John H Goodband, Devi Putra, John A Mills, Keith J Burnham

Original citation:
Sahih, A; Haas, O.C.L; Goodband, J.H; Putra, D; Mills, J.A. and Burnham, K.J. (2006) Respiratory motion prediction for adaptive radiotherapy. Paper given at the IAR Annual meeting, Nancy France

http://www.acd-2006.cran.uhp-nancy.fr/

This conference paper is available to view from the Université Henri Poincaré de Nancy IAR website at: http://www.acd-2006.cran.uhp-nancy.fr/Files/IAR/p14.pdf

RESPIRATORY MOTION PREDICTION FOR ADAPTIVE RADIOTHERAPY

Abdelhamid Sahih [*] **Olivier C L Haas** [*] **John H Goodband** [*]
Devi Putra [*] **John A. Mills** [**] **Keith J. Burnham** [*]

[*] *Control Theory and Applications Centre, Coventry University, CV1 5ED, UK*
[**] *University Hospitals Coventry and Warwickshire NHS Trust, Coventry CV2 4ED*

Abstract: Adaptive and image guided radiation therapy aims to adapt radiotherapy treatment delivery to tumour and patient motion. To achieve this it is necessary to predict trajectory evolution for a time horizon long enough to facilitate the required changes in radiation delivery. This paper presents a new comparative study between different approaches, namely interactive multiple models (IMM), Kalman filter (KF) assuming constant velocity (CV) and constant acceleration (CA) and adaptive bilinear filter (ABF) models and two structures of neural network (NN); a time series prediction (TSP) multi-layer perceptron (MLP) and generalised regression neural network (GRNN), with four different training algorithms. As opposed to existing studies, all algorithms are compared using the same data and new criteria is introduced to demonstrate potential issues with the various algorithms.

Keywords: Adaptive radiotherapy, Bilinear filter, Respiratory modelling, Prediction methods, Kalman filter, Neural networks.

1. INTRODUCTION

Adaptive radiation therapy (ART) is a novel radiotherapy technique developed in order to track and compensate for tumour and patient motion. The motivation for the development of such a technique is that if the cancerous cells can be targeted more effectively, then it will be possible to reduce the treatment margins, hence to a reduction of dose absorbed by the healthy tissues. The approaches currently adopted involve medical imaging or external stereoscopic cameras. Diagnostic fluoroscopy can be used to detect the location of fiducial gold markers surgically implanted onto patients and imaged at a sampling frequency of 30 Hz (Shirato *et al.*, 2000). External markers can be attached or positioned onto the patient and then imaged using systems such as the $Polaris^{TM}$ which is able to provide marker position with a maximum sampling frequency of 30Hz. One such method was developed in Virginia Commonwealth University (VCU), USA, where 24 adult patients with lung cancer were observed over a period of a year, a collation being made of 331 4-minute breathing traces of respiratory motion in anterior-posterior (AP) direction. These published data are used as a basis to compare the methods developed in this work. Although some patient movement during treatment can be limited by the use of suitable constraints, if tumour movement is caused by respiration, either directly, (lung cancer), or indirectly (structures within the thorax and abdomen) the problem becomes less tractable. Indeed, motion due to breathing, although cyclic, is asymmetric and, can be, to some extent, unpredictable by the very nature of the illness. In addition unpredictable patient position changes can cause errors in the tracking.

Assuming that the tracking of tumour motion is achievable, the position of the markers is then fed back

to the radiotherapy equipment to take corrective action. Two alternative actuators have been employed to attempt to keep the relative position of the beam with respect to the organ fixed. A multiple leaf collimator (MLC) can shape the beam exiting the linear accelerator and thus adapt to both motion and shape changes along the longitudinal and the lateral directions. A patient support system (PSS), onto which the patient is positioned, can be used to adapt to the motion in three dimensional space, adding the ability to adjust to AP organ motion.

The main problem faced by manufacturers is that there are a number of latencies and delays in the feedback system. Both the MLC and PSS are electromechanical devices with limited response time (0.12s to 0.33s). Imaging systems require time to process the data and transmit the position of the markers. Delays ranging from 0.03s to 0.09s have been reported in the literature. The computation of the control action, combined with the safety criticality checks that have to be performed at each time sample, means that control loops are sampled in the order of 125 to 200 ms. The combination of the above effect means that by the time the MLC or PSS reaches the desired position, the organs may have moved. There is therefore a need to predict 0.2s to 0.4s in advance the motion of the organ to be tracked.

Current prediction schemes have been performed on regular motion. The most widely accepted model to describe cyclic organ motion is expressed as follows: $z(t) = A_0 - A\cos^{2n}(\frac{\pi t}{\tau} - \phi)$ (Lujan *et al.*, 1999). An average model of the tumour trajectory observed during a patient breathing cycle was used in (Neicu *et al.*, 2003). In the latter, treatment is interrupted if the breathing pattern changes to the extent of falling outside pre-determined gating parameters. In addition to the use of fixed models, aimed to describe the motion more than to predict their evolution accurately, some adaptive models have been developed: adaptive linear filter (Murphy *et al.*, 2002; Vedam *et al.*, 2004), adaptive sinusoidal filter (Vedam *et al.*, 2004), linear autoregressive predictive filter models (Liu *et al.*, 2003). Sharp in (Sharp *et al.*, 2004), compared linear filtering, linear prediction, KF and a fixed TSP MLP NN. It was found that the NN scheme offered the best performances. To adapt to changes in organ motion, an adaptive TSP MLP was developed in (Isaksson *et al.*, 2005) and an adaptive neuro fuzzy inference system (ANFIS) was proposed in (Kakar *et al.*, 2005).

The difficulty associated with comparing the performance of all these algorithms is that they use different data sets or different data within the same data set and restrict the applicability of their approaches to regular motion, which are in practice rarely achieved by patients. Further, the most widely used criterion to evaluate the performance of such prediction algorithms is the root mean square error (RMSE) for each trajectory or the mean of the RMSE when more than one trajectory is considered. Such criteria do not, however, highlight algorithms that may fail for short periods of time and hence exhibit infrequent large errors. To account for large error, whilst at the same time preventing noise from the imaging equipment to interfere with the results, filtered measurements and predicted signals are used and then the maximum error is calculated.

A refinement of the approach given in (Sahih *et al.*, 2005) is proposed where an ABF model used for prediction is estimated by the means of a regularization technique at each filter iteration. This approach is compared to a previously developed IMM filter algorithm (Putra *et al.*, 2006) which is different to that of (Sharp *et al.*, 2004) in that it is based on linear stochastic models with the sampling period being the only parameter in the system matrices. Whilst many NN schemes have been developed, no attempt has been made to justify the use of training algorithms nor the practicality associated with their need for on-line updating. This paper compares three training algorithms for a TSP MLP and a GRNN which is a modification of the standard Gaussian radial basis function (GRBF) designed to facilitate approximation for system modelling and prediction.

2. PREDICTION METHODS

2.1 KF and IMM

The KF is an optimal linear estimator that minimizes the mean of the square error, which was introduced by (Kalman, 1960). Since then, the KF has been a subject of extensive research and application, particularly in the area of autonomous navigation, see for example (Grewal and Andrews, 1993). The recursive feature of the KF makes it suitable for on-line prediction. In order to use the KF and the IMM filter to predict tumour motion, dynamic models of such motion are required. Two stochastic linear models and a hybrid combination of them, which are suitable for use in both the KF and the IMM filter were proposed in (Putra *et al.*, 2006). The first model is a CV model of the form:

$$\begin{bmatrix} x1(k+1) \\ x2(k+1) \end{bmatrix} = \begin{bmatrix} 1 & \Delta t \\ 0 & 1 \end{bmatrix} \begin{bmatrix} x1(k) \\ x2(k) \end{bmatrix} + \begin{bmatrix} \Delta t \\ 1 \end{bmatrix} v(k)$$
$$y(k) = \begin{bmatrix} 1 & 0 \end{bmatrix} x(k) + w(k)$$

where x_1 and x_2 denote, respectively, the position and the velocity of the tumour, Δt the sampling period, y the measured tumour position, v and w the process and measurement noises that are assumed to be uncorrelated zero-mean Gaussian white noise sequences with covariance matrices Q and R, respectively. The second model is a CA model

$$\begin{bmatrix} x1(k+1) \\ x2(k+1) \\ x3(k+1) \end{bmatrix} = \begin{bmatrix} 1 & \Delta t & \Delta t^2 \\ 0 & 1 & \Delta t \\ 0 & 0 & 1 \end{bmatrix} \begin{bmatrix} x1(k) \\ x2(k) \\ x3(k) \end{bmatrix} + \begin{bmatrix} \Delta t^2 \\ \Delta t \\ 1 \end{bmatrix} v(k)$$

$$y(k) = \begin{bmatrix} 1 & 0 & 0 \end{bmatrix} x(k) + w(k)$$

which is an extension of the CV model obtained by including the acceleration denoted by $x3$. It is important to note that the noise v is added to allow the changing of direction of the velocity and the acceleration such that the model is able to replicate both regular and irregular motions of the tumour. However, the CV and CA models are only valid for relatively small time steps, i.e. $0 < \Delta t < 0.5s$, because linear motions are assumed. It was shown in (Putra *et al.*, 2006) that a single CV or CA model employed in isolation gave inferior results when compared to the IMM scheme combining both models. For a description of the approach see (Putra *et al.*, 2006).

2.2 ABF approach

Respiratory motion modelling can be achieved by considering the lung as an ABF which replicates the respiratory motion in response to an input signal generated by the nervous system (see Figure 1). In this work such an input signal is modelled as a square wave which corresponds to regular switching between the inhale and exhale phases.

Bilinear systems form a class of nearly linear systems which differ from those generally used in that the gain and time constant are input dependent quantities. The bilinear terms correspond to weighted products between the input and the output of the system. The choice of a bilinear model stems from the realization that the dynamics of the respiratory motion is different in the inhale and the exhale phases, i.e the response is asymmetric. The approach aims to generate an input signal which is repeatedly triggered to coincide with the on-set of inhale and exhale. The switching levels of the input signal are fixed. The signal is then used as an assumed input signal to an ABF model which is recursively estimated on-line.

Having analysed the respiratory motion, it has been found that both exhale and inhale phases can be approximated with a second order system response. Thus, the following second order ABF structure has been chosen to model the respiratory motion:

$$y_k = -a_0^k y_{k-1} - a_1^k y_{k-2} + b_0^k u_{k-1} + \eta_0^k y_{k-1} u_{k-1} \quad (1)$$

The regression model can be expressed as $y_k = \varphi_k \theta_k$, where $\theta_k = [a_0^k, a_1^k, b_0^k, \eta_0^k]^T$. The regressor is given by $\varphi_k = [-y_{k-1}, -y_{k-2}, u_{k-1}, y_{k-1}u_{k-1}]$.

Assuming that the frequency of breathing is known and the position of the organ is acquired in real time by the measurement tool, the steps of modelling and prediction are given as follows:

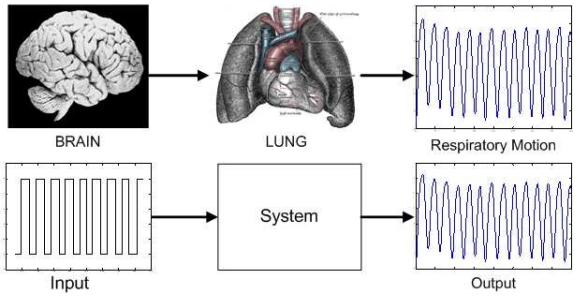

Fig. 1. Illustrating the modelling principle of ABF.

(1) Given $\{y_{k-1}, y_{k-2}, ..\}$ and $\{u_{k-1}, u_{k-2}, ..\}$ the one step ahead prediction is : $\widehat{y}_k = \varphi_k \theta_k$
(2) The prediction errror at step k is:

$$\varepsilon_k(\theta_k) = y_k - \widehat{y}_k = y_k - \varphi_k \theta_k \quad (2)$$

(3) Estimate the parameters of the ABF:

$$\theta_k^* = \underset{\theta}{\operatorname{argmin}} \{\varepsilon_k(\theta_k)\}^2 \quad (3)$$

subject to $0 < p_{1,2} < 1$, where $p_{1,2}$ are the poles of the linear part of the filter.
(4) Use the actual model to predict h steps ahead.

The approximate ABF expressed in discrete-time is given by :

$$\frac{b_0 z}{z^2 + (a_0 - \eta_0 u_\alpha) z + a_1}$$

Alternatively,

$$\frac{b_0 z}{(z - p_1)(z - p_2)}, where \;\; p_{1,2} = f(\theta, u_\alpha)$$

The equivalent poles of the system can (loosely) be expressed in term of filter parameters:

$$(a_0 - \eta_0 u_\alpha) = -(p_1 + p_2)$$
$$a_1 = p_1 p_2$$

where u_α is the known value of the input signal and p_1, p_2 are the poles of the system. The parameters of the filter can be estimated by minimizing the squared prediction errors. This can lead to several solutions, including those which correspond to an unstable filter. To ensure that the filter remains stable, an optimization technique with constraints has been used. This is equivalent to applying regularization technique, by constraining the parameters to be bounded on an interval.

2.3 Neural Network

NNs provide proven methods for synthesizing nonlinear input-output mappings, and have been used in predictive control (Haykin, 1999). A supervised NN *learns* a mapping through training data, which is repeatedly presented. Two different NN structures are investigated: a MLP and GRNN. A predicted marker

position at a point x, and h steps ahead of step k is given by:

$$\widehat{x}(k+h) = F\{x(k), x(k-1), ..., x(k-n)\} \quad (4)$$

where F is a nonlinear function described by the NN and n is the number of past positions used in combination with the present input $x(k)$ to determine the future position. The required NN has $(n+1)$ inputs, 1 output and a hidden layer, the approximate size of which is optimised using the training data.

MLP design and training

The MLP uses an iterative algorithm to change parameter weights which act upon connections between the neurons. In the present work, a comparison is made between the following MLP training schemes: i) conjugate gradient back-propagation (CGBP) (Fletcher, 1987)- used in (Sharp *et al.*, 2004), ii) Levenberg-Marquart (LM) algorithm (Levenberg, 1944; Marquardt, 1936)- used in (Isaksson *et al.*, 2005) and iii) Bayesian regularisation (BR) off-line to minimize the number of network parameters followed by conjugate gradient back propagation CGBP for on-line updating. Applying a method, similar to that of (Sharp *et al.*, 2004), the NN training was initially performed off-line. The TSP MLP architecture is created by selecting the first 20 s of data, 16 s being used to training and 4 s for validation from a random number of 30 traces out of the 331 internal markers traces. The number of MLP inputs and hidden neurons are increased incrementally, starting with one of each until there is no improvement in the validation mean square error (MSE)

$$MSE_{val} = \frac{1}{N}\sum_{i=1}^{N}(\mathbf{t}_i^{val} - \mathbf{y}_i)^T(\mathbf{t}_i^{val} - \mathbf{y}_i), \quad (5)$$

where $\mathbf{t}_i^{val}$ is a target vector from the validation set vector, $\mathbf{y}_i$ a training output vector, and N the number of input-target data pairs. This procedure is carried out with early stopping to ensure good generalisability. To enable the NN to adapt to patients inter and intra variability, further updating was carried out on-line. During the first 20s, data is recorded and used to re-train the NN for each patient. Again the CGBP and LM use 16 s of data for training and 4s for validation, whilst BR uses the 20 s for training. Following this initial training, the NN is updated every 1s. The time required to update the NN was found to be 0.1s when the latest 5s of data are used. The validation is performed by selecting one point every 5 samples (i.e. 20% of data set). Note that (Kakar *et al.*, 2005) assume that updating can be performed at each iteration, however, in this study, this would incur too great a computational cost on the overall tracking scheme. Typically MLP training is facilitated by re-scaling the inputs. But this approach assumes that the range of motion must be known in advance. This is true in case of fairly regular motion, but fails in the case of irregular motion where the patient may shift position before breathing regularly again. The approach adopted in this study does not limit the possible set of inputs and as such the prediction determined using MLP cannot be guaranteed to be bounded. However, the MLP can adapt to significant trajectory changes.

GRNN design and training

The vector, $\mathbf{c}_k, k = 1, 2, ..., M$ defines the centre of the k^{th} GRBF and is given by an input vector from the training set, and each weight w_j is the target associated with the respective input vector i.e $w_j = t_j$. The h step ahead predicted output $\widehat{x}(k+h)$ of the GRNN is given by

$$\widehat{x}(k+h) = \frac{\sum_{j=1}^{N} w_j g(\mathbf{x}; \mathbf{c}_j)}{\sum_{j=1}^{N} g(\mathbf{x}; \mathbf{c}_j)} \quad (6)$$

where $g(\mathbf{x}; \mathbf{c}_j) = \exp(-\|\mathbf{x} - \mathbf{c}_j\|^2/\sigma_j^2)$, represents a Gaussian activation function and σ_j is the standard deviation of the Gaussian function g. It can be shown that the magnitude of the GRNN output is bounded by the size of the maximum value of $w_j = t_j$ such that

$$|\widehat{x}(k+h)| \leq \max_{\mathbf{x}} |w_j| \quad (7)$$

The GRNN is constructed using centres selected at every 5^{th} point in the training data $\equiv 6$ Hz i.e. using the same data points as those used for validation purposes with the TSP MLP. The fastest human breathing cycle frequency is ≈ 2 Hz. During RT treatment, frequencies are generally maintained between 0.25 and 0.5 Hz . Sampling at 6 Hz ($> 2 \times 2$ Hz) therefore ensures that aliasing does not occur. The number of GRNN inputs is first assessed using a similar procedure to that used with the TSP MLP. The standard deviation of the GRBF neurons constituting the hidden layer is calculated for each change in the number of inputs using $\sigma = \frac{d_{max}}{\sqrt{M}}$, where d_{max} is the maximum Euclidian distance between $\mathbf{x}$ and $\mathbf{c}_j(\|\mathbf{x} - \mathbf{c}_j\|)$, and M the number of GRBFs (hidden neurons) chosen for the network, here $M = 30$. Having obtained the number of inputs, the GRBF width is then *optimised* for each data set by iteratively calculating the GRNN response to validation data for several width values. Limiting the calculation time to 20 s (100 calculations), the training commences with the initial value $\sigma_0 = \frac{d_{max}}{\sqrt{M}}$ and the value of σ is increased in steps of $\frac{\sigma_0}{20}$ until there is no improvement in mean squared error.

3. RESULTS AND DISCUSSION

The performance of the algorithms presented in this work have been tested using a clinical data set from VCU. Results are given in Table 1 and Table 2. The effectiveness of the algorithms are compared to the case of no prediction, i.e. the target is assumed to remain in the same position. This is equivalent to

shifting the current trajectory by h steps ahead, where h is the prediction horizon. Unlike the NN schemes and the ABF, the Kalman CA, CV and IMM algorithms require sampling the data at the same period as the prediction horizon. It was found that all the predictors perform consistently, achieving a reduction of the RMSE compared to no prediction. In terms of RMSE, the Kalman CV gave the best results for both short and long time prediction. A comparison between the NN schemes shows that the new hybrid algorithm combining BR and CGBP produces the best average RMSE results. For a sampling period below 0.5 s, most NN approaches were found to perform similarly. However, for longer sampling period, BR produces better results for all three latencies investigated, see Figure 2.

In radiotherapy treatment and for safety reasons, it is very important to have a small maximum error, to avoid the a radiation of healthy tissues. As shown in Figure 3, the prediction error can be large either in the beginning of inhalation or end of exhalation as well when a large variation in position occurs, which cannot be assessed by RMSE. This has prompted the introduction of new (in the context of ART) criteria to assess the performance of prediction algorithm. These criteria are based on the maximum error for each trajectory and the average of the maximum error for all trajectories. Analyzing the difference between the predicted trajectories and the actual marker position for the Kalman CA, CV and IMM has highlighted that the largest errors occurred around the transition between the inhale and the exhale phases. However, significantly better accuracy could be achieved during the inhale and exhale phases. For long time prediction, the ABF gave a small maximum prediction error compared to the Kalman CV, however it is assumed that the transitions between inhale and exhale phases are known. In practice these transitions can be estimated using a Kalman filter. NN schemes are limited by the fact that the large errors (see Figure 3), can only be captured once the NN have been updated.

	Error criteria [mm]		
Methods	$\overline{RMSE}$	Std. of RMSE	$\overline{\lvert e^{max} \rvert}$
No Predict.	1.29	0.51	3.00
Kalman CV	**0.19**	**0.11**	**0.72**
Kalman CA	0.34	0.17	1.05
IMM	0.30	0.15	0.94
ABF	0.29	0.13	0.78
CGBP	0.63	0.54	3.18
GRNN	0.77	0.16	5.25
LM	0.76	5.23	40.82
BR+CG	0.48	0.54	3.08

Table 1. Comparative study using 331 trajectories for 0.2s ahead prediction (the best results are indicated in bold).

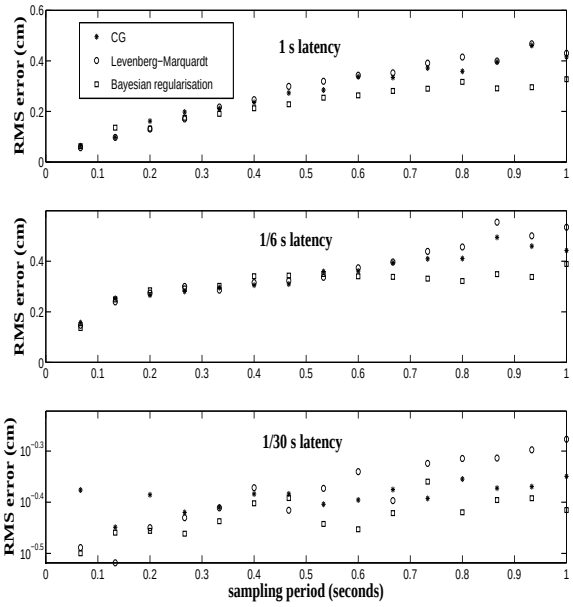

Fig. 2. Illustrating the modelling principle RMS error of marker positions as a function of sampling period for (top) 1 s latency, (middle) 1/6 s latency and (bottom) 1/30 s latency.

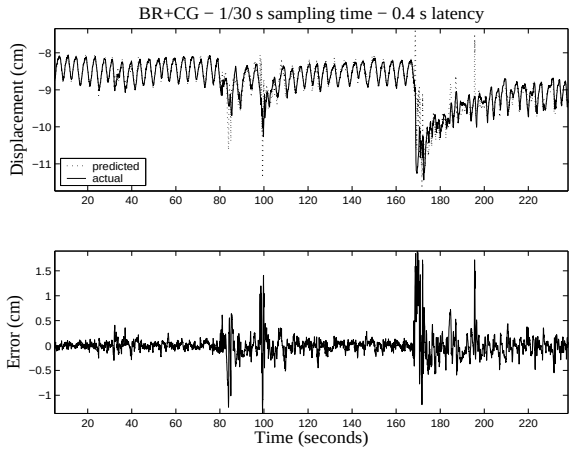

Fig. 3. Illustrating (top) the real and predicted signal, (bottom) a typical error levels for 0.4s ahead prediction using BR+CGBP.

	Error criteria [mm]		
Methods	$\overline{RMSE}$	Std. of RMSE	$\overline{\lvert e^{max} \rvert}$
No Predict.	2.54	1.00	5.83
Kalman CV	**0.78**	**0.44**	2.84
Kalman CA	1.15	0.58	3.45
IMM	1.08	0.55	3.25
ABF	0.85	**0.44**	**2.25**
GRNN	1.69	0.50	4.35
CGBP	1.20	0.93	5.03
LM	1.61	8.40	66.56
BR+CG	0.97	0.78	5.66

Table 2. Comparative study using 331 trajectories for 0.4s ahead prediction (the best results are indicated in bold).

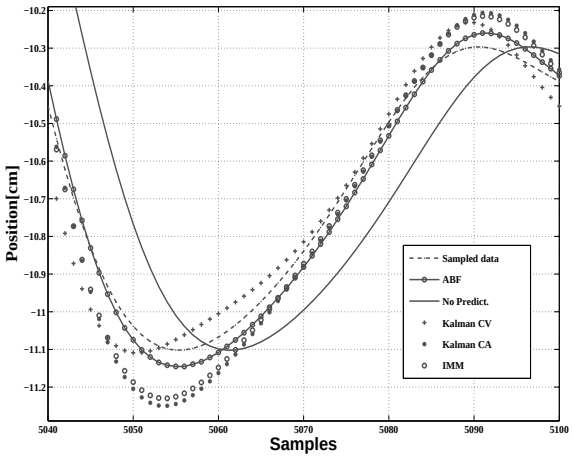

Fig. 4. Illustrating the 0.2s ahead prediction using ABF, IMM, Kalman CV and CA against no prediction and sampled data for trajectory No. 1.

4. CONCLUSIONS AND FURTHER WORK

This study has presented different approaches to predict tumour motion described by external markers: i) methods based time series prediction: NNs, Kalman CV, Kalman CA, IMM. ii) method based system identification: ABF. It has been demonstrated that the use of regularization for ABF and NN (for low sampling frequency) improves prediction performance. A hybrid system of different predictors such as BR+CG can also improve the prediction. It was found that changes in the motion can lead to a large prediction error, and the healthy tissues can consequently be irradiated. This requires the maximum prediction error to be taken into account in the criterion to minimized. Future work will include investigation of hybrid systems which combine Kalman CV and ABF to reduce this prediction error.

ACKNOWLEDGEMENTS

This work is sponsored by the Framework 6 European integrated project Methods and Advanced Equipment for Simulation and Treatment in Radiation Oncology (MAESTRO) CE LSHC CT 2004 503564. The Authors are thankful to the Physics staff at the University Hospitals Coventry and Warwickshire NHS Trust for their help and to the VCU, for providing organ motion data.

REFERENCES

Fletcher, R (1987). *Practical methods of optimization*. 2nd edition, New York: Wiley.

Grewal, MS and AP Andrews (1993). *Kalman Filtering:Theory and Practice*. Prentice Hall.

Haykin, S (1999). *Neural Networks: A Comprehensive Foundation*. 2nd ed, Prentice-Hall Inc.

Isaksson, M, J Jalden and MJ Murphy (2005). On using an adaptive neural network to predict lung tumor motion during respiration for radiotherapy applications. *Medical Physics* pp. 3801–3809.

Kakar, M, H Nystrom, LR Aarup, TJ Nøttrup and DR Olsen (2005). Respiratory motion prediction by using the adaptive neuro fuzzy inference system (anfis). *Physics In Medicine And Biology* **50**, 4721–4728.

Kalman, RE (1960). A new approach to linear filtering and prediction problems. *Transactions of the ASME: Journal of Basic Engineering,* **82**, 35–45.

Levenberg, K (1944). A method for the solution of certain problems in least squares. *Quarterly Journal on Applied Mathematics* **2**, 164–168.

Liu, H, Y Yu, D Wo and M Schell (2003). A prospective tracking algorithm for motion compensation radiotherapy. In: *the American Association of Physicists in Medicine: Annual meeting*. San Diego.

Lujan, AE, EW Larsen, JM Balter and RTK Haken (1999). A method for incorporating organ motion due to breathing into 3D dose calculations. *Medical Phyisics* **26**(5), 715–720.

Marquardt, DW (1936). An algorithm for least-squares estimation of non-linear parameters. *Journal of the Society for Industrial and Applied Mathematics* **11**, 431–441.

Murphy, MJ, D Martin, R Whyte, J Hai, C Ozhasoglu and Q Le (2002). the effectiveness of breath-holding to stabilize lung and pancreas tumors during radiosurgery. *International Journal of Radiation Oncology Biology Physics* **53**(2), 475–482.

Neicu, T, H Shirato, Y Seppenwoolde and SB Jiang (2003). Synchronized moving aperture radiation therapy (smart): average tumour trajectory for lung patients. *Physics in Medicine and Biology* **48**, 587–598.

Putra, D, OCL Haas, JA Mills and KJ Burnham (2006). Prediction of tumour motion using interacting multiple model filter. In: *Proceedings of the 3rd IEE International Conference on Medical Signal and Information Processing (MEDSIP)*. Glasgow.

Sahih, A, OL Haas, KJ Burnham and J Mills (2005). Organ motion modelling and prediction for adaptive radiotherapy. In: *Proc. IAR-ACD*. Vol. 2. Mulhouse, France. pp. 211–216.

Sharp, GC, SB Jiang, S Shimizu and H Shirato (2004). Prediction of respiratory tumour motion for real-time image-guided radiotherapy. *Physics in Medicine and Biology* **49**, 425–440.

Shirato, H, S Shimizu and K Kitamura (2000). Four dimensional treatment planning and fluoroscopic real time tumor tracking radiotherapy for moving tumor. *nternational Journal of Radiation Oncology Biology Physics* **48**(2), 435–442.

Vedam, SS, P. Keall, A. Docef, D. Todor, V. Kini and R. Mohan (2004). Predicting respiratory motion for four-dimensional radiotherapy. *Medical Physics* **31**(8), 22–74.